

Low-dc-field susceptibility of CuMn spin glass

Shoichi Nagata,* P. H. Keesom, and H. R. Harrison

Department of Physics, Purdue University, West Lafayette, Indiana 47907

(Received 7 August 1978)

Low-dc-field magnetic-susceptibility measurements are reported for CuMn alloys containing 1.08- and 2.02-at.% Mn using a superconducting quantum-interference device. The zero-field cooled initial susceptibility shows a cusplike peak at T_g , the transition temperature to a spin-glass state. After field cooling from $T > T_g$ (even for $H=2$ G), the susceptibility below T_g is nearly independent of temperature with the constant value of $\sim 0.97\chi(T_g)$. The high-temperature susceptibility follows a Curie-Weiss law until just above T_g ; the value of the Curie temperature is very small. Using the theory of Sherrington and Kirkpatrick, the spin-glass order parameter $q(T)$ is extracted from the susceptibility data. A critical index $\beta=1$ is obtained assuming a power law for $q(T) \propto (1-T/T_g)^\beta$. The results are qualitatively in agreement with the prediction of an Edwards-Anderson-type mean-field theory.

I. INTRODUCTION

The investigation of spin glasses like CuMn or AuFe during the last six years suggests that the magnetic ions form a new magnetic phase below a temperature T_g . Below T_g the magnetic moments are frozen in random orientations without a conventional long-range order. It is well known that the low-ac-field magnetic susceptibility of a spin glass or micromagnet has a sharp cusplike peak at the temperature T_g which indicates a cooperative, but random, freezing of magnetic moments.¹ In the temperature region below T_g irreversible magnetic behavior is observed, which depends on the magnetic history of the specimen, e.g., whether or not the sample was cooled through T_g in an external field.

The present work is concerned with the low-dc-field susceptibility of CuMn spin glass. In analogy to ferromagnetism, we will use an initial susceptibility χ_i for the susceptibility of the sample when it is cooled in the absence of a magnetic field and thereafter the measuring magnetic field is applied; after application of this field the sample temperature is not allowed to decrease. The symbol χ_h will be used if the measuring field is applied above T_g . The initial susceptibility χ_i and the susceptibility χ_h have been measured between 4.2 and 50 K. Tholence and Tournier² as well as Guy³ have already discussed the effect of magnetic history on another spin glass, AuFe, and the difference in results between the dc static measurement and the ac measurement.

Edwards and Anderson⁴ (EA) proposed that spin correlations between Gibbs-like replicas of the random system play the role of a spin-glass order parameter. Sherrington and Kirkpatrick⁵ obtained a spin-

glass solution characterized by the EA order parameter $q(T)$. Using this theory, Mizoguchi *et al.*⁶ extracted $q(T)$ from the observed susceptibility for Gd_{0.37}Al_{0.63}. We obtained the order parameter for CuMn following this analysis. The susceptibility χ provides an experimental probe of $q(T)$, since⁵

$$\chi(T) = \{C(T)[1 - q(T)]\} \times \{T - \Theta(T)[1 - q(T)]\}^{-1} \quad (1)$$

In the mean-field theory,^{5,6} $C(T)$ and $\Theta(T)$ are constants and are the Curie constant and the Curie temperature, respectively.

Recently, Binder⁷ has discussed the spin-glass problem in a brief review. New experimental data,⁸ such as the anomalous thermal expansion of CuMn and MgMn, have been observed and it is our hope that the measurements presented below will be helpful.

II. EXPERIMENTAL

A. Sample

Single crystals of CuMn were grown in the Central Materials Preparation Facility of Purdue University. The elements (99.995% Cu and 99.9% Mn) were first melted in a 99.8% alumina crucible to make a "mother alloy" containing about 5-at.% Mn. Pieces of the mother alloy were diluted with appropriate amounts of pure Cu in a slightly tapered graphite (maximum 0.06-wt.% ash content) crucible, and were grown into single crystals by the Bridgman technique using rf induction heating. All melting was done under an

atmosphere of gettered Ar. Etching of the resulting single crystals ($\frac{1}{4}$ -in. diam), which had a few small surface grains, revealed striations or cell structure with a spacing on the order of 0.01 cm, so they were homogenized at 1000°C for 3 days in an evacuated fused silica ampoule to remove this structure. After reetching, parallelepipeds of single-crystalline material (3.0×2.2×1.7 mm) were cut from the boule with a low-speed diamond wheel saw. These parallelepipeds were etched again, to remove the strained surface due to cutting. They were then reencapsulated in evacuated fused silica ampoules and given a second heat treatment for 1 hr. at 1000°C, and then quenched in ice water. Magnetic measurements were performed immediately after this treatment to avoid room-temperature aging complications.

B. Susceptibility measurements

A superconducting magnetometer was constructed. Detailed discussions of superconducting magnetometers using an rf-SQUID (superconducting quantum-interference device) have appeared in the literature.⁹⁻¹⁵ The magnetic flux sensor of such a magnetometer is a pair of astatically wound superconducting-coils coupled to a rf-SQUID. If a sample is placed inside one of the two coils, a change in its magnetization is sensed by the SQUID and the output is used to drive the Y coordinate of an X-Y recorder. The sample (S) and a sample holder (H) are placed inside a chamber (C) together with a small amount of exchange gas. This system (S, H, and C) was placed inside a vacuum can. The temperature could be raised with the help of a heater glued onto the chamber. A germanium thermometer on C indicated the temperature. The potential drop over the thermometer drives the X axis of the X-Y recorder so that a continuous record of the change in magnetization of the sample versus temperature is obtained. The sample holder and chamber as well as the vacuum container are made of pure copper. By placing the pair of astatically wound coils symmetrically with respect to all three, the change in background magnetization was minimized. The magnetic field is supplied by a superconducting magnet operated in the persistent mode to provide a stable magnetic field.

The sample, a small parallelepiped, described above, was mounted and nearly filled a square slot machined into the sample holder. In that same slot, about 2 mm from the sample, was also mounted a needle-shaped piece of Pb or Ta (approximately 0.5 mg) with the length axis parallel to the field applied by the superconducting magnet. This piece of Pb or Ta gave a very sharp change in magnetization at its transition from superconducting to normal state, or vice versa. The magnitude of this change calibrated

the sensitivity of the system, while the transition temperature of Pb or Ta gave the magnitude of the applied field.

The background change in magnetization was measured with an empty sample holder at all fields and temperatures. It was impossible to determine an absolute value of the magnetization, as only differences were measured. However, the data were observed to follow very nearly a $1/T$ dependence at high temperatures ($T > 40$ K). We assumed that this dependence would hold to $1/T=0$, and the $1/T=0$ intercept was taken as the "zero" value of the magnetization. The system was constructed so as to eliminate spurious signals from vibrations, magnetic radiation, and the paramagnetic background of the construction materials. For this system the sensitivity is sufficient to detect changes 2×10^{-9} emu in susceptibility in a field 5 G.

III. RESULTS AND DISCUSSION

The susceptibilities deduced from the magnetization measured by a low-field static method are shown in Fig. 1 for $\text{Cu}_{0.9892}\text{Mn}_{0.0108}$ and $\text{Cu}_{0.9798}\text{Mn}_{0.0202}$. Initial susceptibilities (b) and (d) were measured in a field of 5.90 G, after cooling the samples to the lowest temperature in zero field (less than 0.05 G). Cusplike peaks are observed at the temperatures T_g of 9.90 and 14.67 K for the compositions 1.08- and 2.02-at.% Mn, respectively. The curves (a) and (c) were also obtained from the magnetization in the field $H=5.90$ G, but for these cases, the field was applied before the samples were cooled below T_g . Between 2 and 25 G, all the susceptibilities of these two samples were magnetic field independent. The susceptibilities χ_i and χ_h have been measured several times under the same conditions and have been reproduced very well. Below T_g the susceptibilities (a) and (c) decreased slowly, flattening out to a constant value of $0.98\chi(T_g)$ and $0.97\chi(T_g)$ for the 1.08- and 2.02-at.%-Mn compositions, respectively. These results agree with Guy³ and Tholence and Tournier² for AuFe and Hirshkoff *et al.*¹⁶ for very dilute CuMn.

Figure 2 shows the initial susceptibilities near the peak temperature T_g . A rounded maximum is seen for the 1.08-at.%-Mn sample while a sharp cusp is observed for the 2.02-at.%-Mn sample. We measured also the susceptibility for a 2.02-at.%-Mn sample which was homogenized but not quenched in order to check for any difference in thermal treatment, but did not detect any.

The high-temperature susceptibility can be expressed by the Curie-Weiss law

$$\chi = C / (T - \Theta) \quad (2)$$

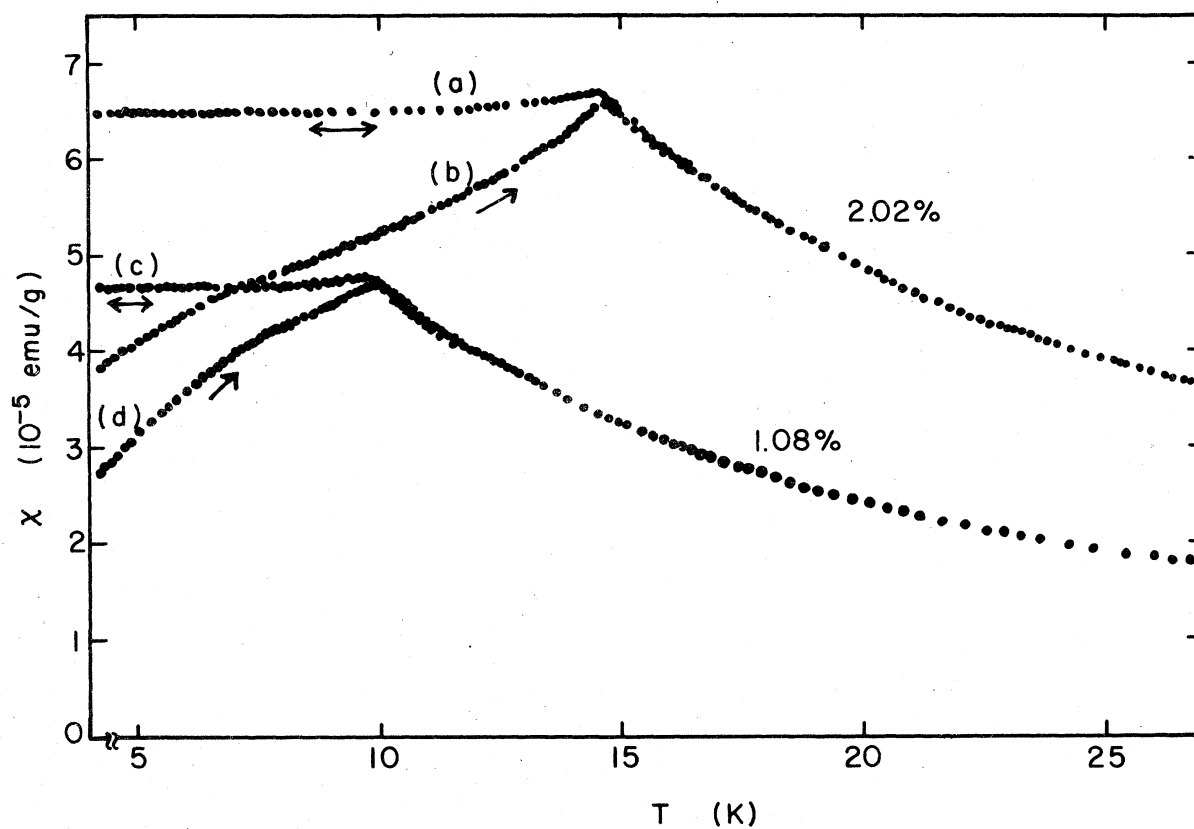


FIG. 1. Static susceptibilities of CuMn vs temperature for 1.08- and 2.02-at.% Mn. After zero-field cooling ($H < 0.05$ G), initial susceptibilities (b) and (d) were taken for increasing temperature in a field of $H = 5.90$ G. The susceptibilities (a) and (c) were obtained in the field $H = 5.90$ G, which was applied above T_g before cooling the samples.

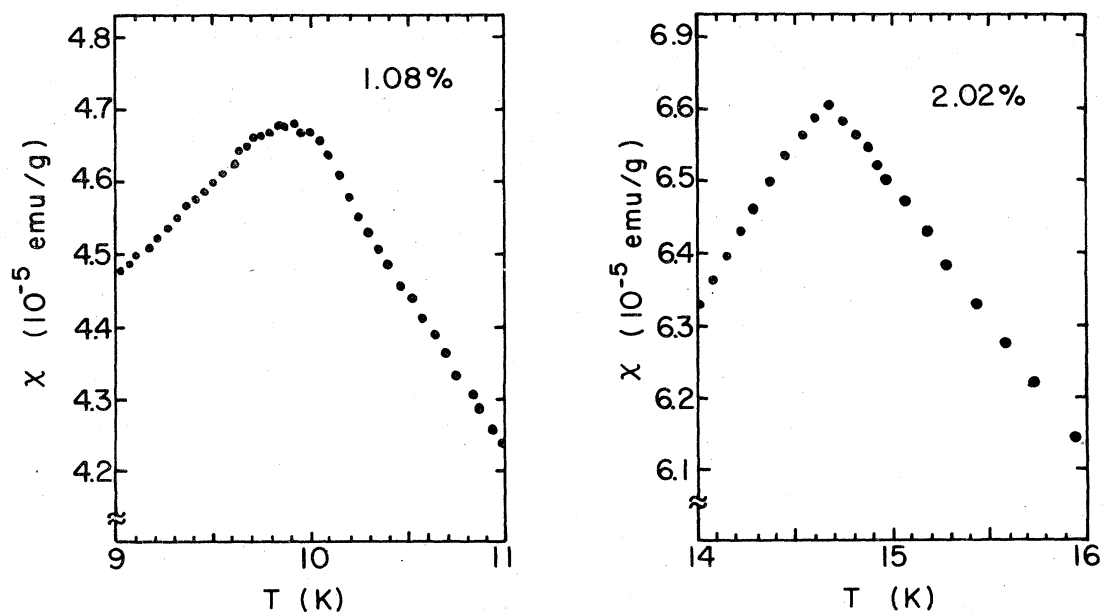


FIG. 2. Initial susceptibilities near T_g for 1.08- and 2.02-at.% Mn.

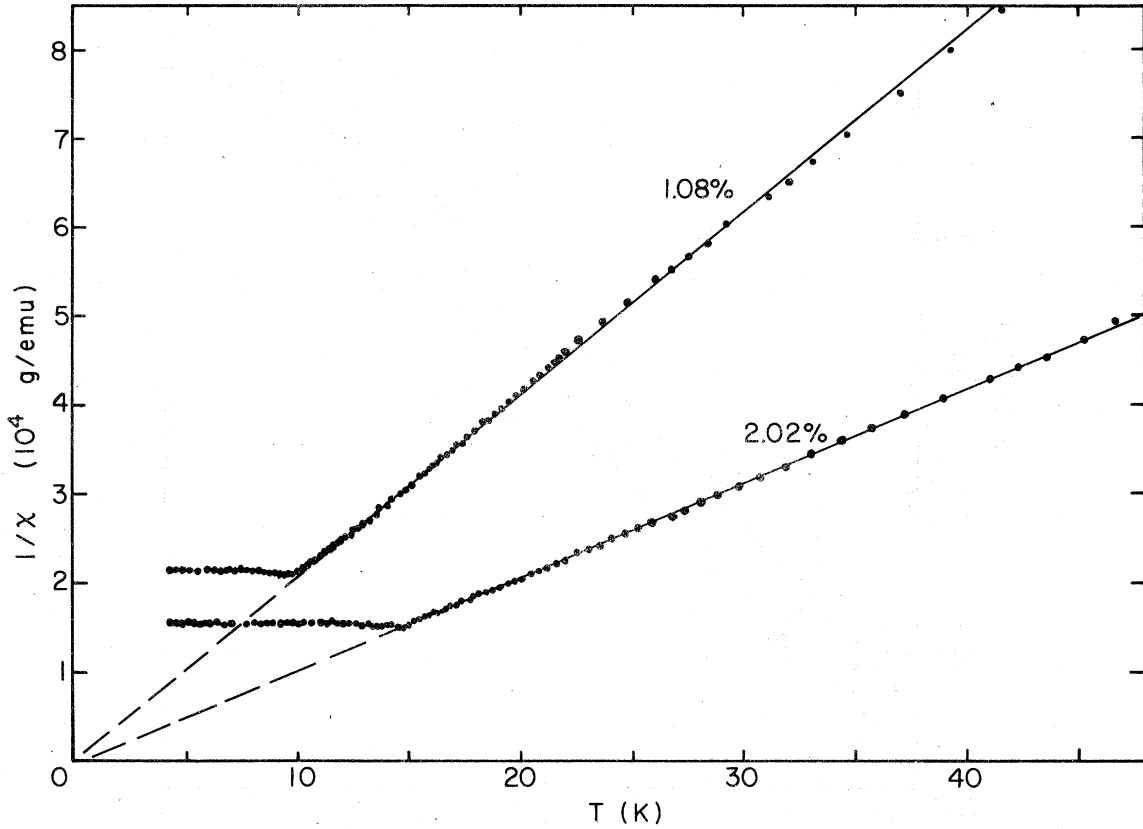


FIG. 3. Inverses of CdMn gram susceptibility $1/\chi$ as a function of temperature, for 1.08- and 2.02-at.% Mn. Each χ follows a Curie-Weiss law until just above T_g . The values of Θ are small ($\Theta \ll T_g$).

The temperature intercept of $1/\chi$ vs T gives the value of the paramagnetic Curie temperature Θ as shown in Fig. 3 and the slope $1/\chi$ yields the effective magnetic moment per Mn atom in Bohr magnetons,

$$P_{\text{eff}} = g[J(J+1)]^{1/2} = \left(\frac{3k_B}{D\mu_B^2 d(1/\chi)/dT} \right)^{1/2}, \quad (3)$$

where J is the angular momentum, μ_B is the Bohr magneton, g is the Landé g factor, and k_B is the

TABLE I. Peak temperature T_g , paramagnetic Curie temperature Θ , and the effective number of Bohr magnetons per Mn atom, for two Mn concentrations.

| Concentration (at.% Mn) | Peak temperature T_g (K) | Paramagnetic Curie temperature Θ (K) | Effective Bohr magneton number P_{eff} |
|-------------------------|----------------------------|---|---|
| 1.08 | 9.90 ± 0.05 | 0 ± 0.5 | 4.80 ± 0.1 |
| 2.02 | 14.67 ± 0.02 | $+0.2 \pm 0.5$ | 4.86 ± 0.1 |

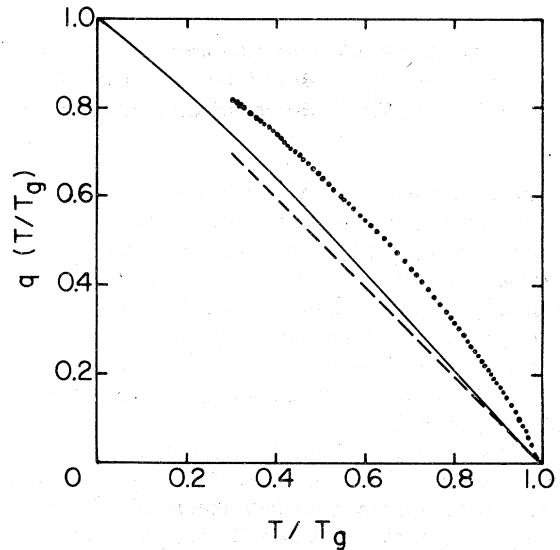


FIG. 4. Spin-glass order parameter $q(T)$ for 2.02-at.% Mn, which is deduced from Eq. (4), as a function of the reduced temperature T/T_g . The dots are obtained from the initial susceptibility, curve (b) in Fig. 1. The dashed line which is a nearly diagonal line shows the result from the susceptibility, curve (a) in Fig. 1. The solid line indicates the mean field theory prediction of Ref. 5.

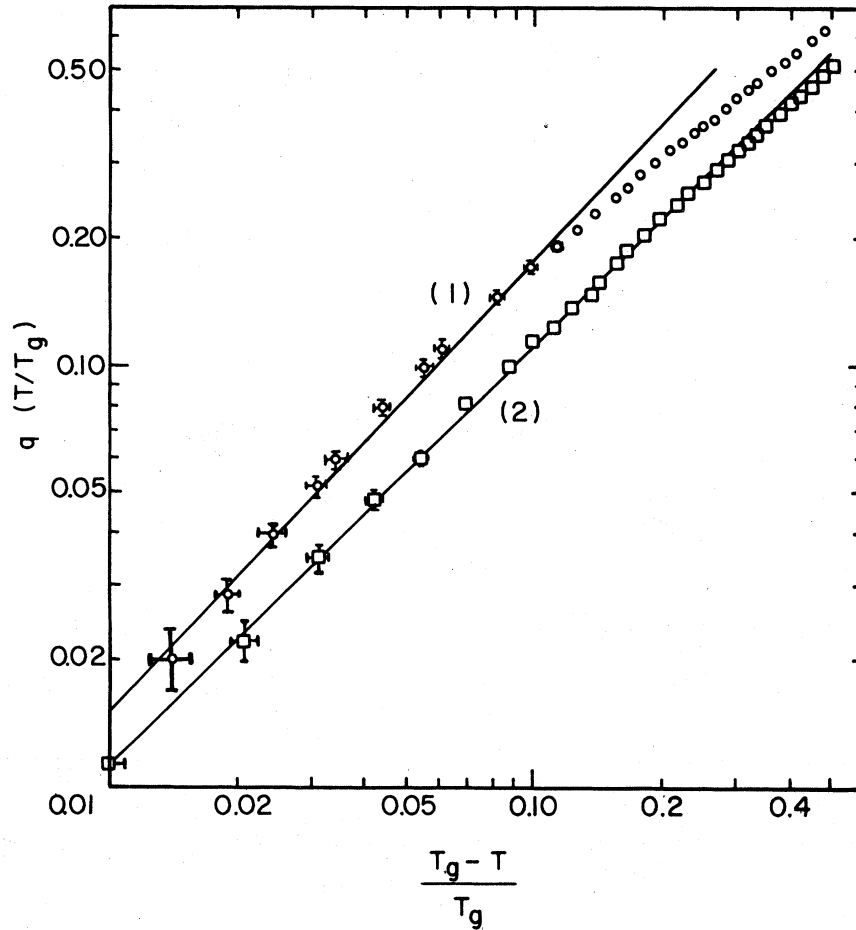


FIG. 5. Log-log plots of the spin-glass order parameter $q(T/T_g)$ vs $(T_g - T)/T_g$ for the 2.02-at.-%-Mn sample. Line (1) shows $q(T/T_g) = 2.1(1 - T/T_g)^{1.07}$, $\beta = 1.07$, which is deduced from the susceptibility (b) in Fig. 1, and (2) indicates $q(T/T_g) = 1.1(1 - T/T_g)^{1.00}$, $\beta = 1.00$, which is deduced from (a) in Fig. 1.

Boltzmann constant. In this calculation χ is in emu/g, and D is the number of magnetic atoms per gram. A summary of the results for CuMn is shown in Table I. The values of P_{eff} are close to the value calculated for Mn^{3+} rather than Mn^{2+} . The paramagnetic Curie temperatures Θ are very small in comparison with T_g ($\Theta \ll T_g$) and the deviations from the Curie-Weiss law are small for each sample until just above T_g .

We followed the method of Mizoguchi *et al.*⁶ to obtain the EA-type spin-glass order parameter $q(T)$, which is based on the mean field theory of Sherrington and Kirkpatrick.⁵ Relation (1) was used to obtain

$$q(T) \cong 1 - T\chi(T)[C + \Theta\chi(T)]^{-1} \quad (4)$$

The value of $q(T)$ was deduced from the susceptibility $\chi(T)$, the Curie constant C , and the Curie temperature Θ . Figure 4 shows $q(T)$ for the 2.02-at.-%-Mn sample. The solid line indicates the mean-field-

theory prediction of Ref. 5. The dots come from curve (b) in Fig. 1 and the broken line, which is nearly a diagonal line, shows $q(T)$ from curve (a) in Fig. 1. In Fig. 5, q is plotted logarithmically versus $(T_g - T)/T_g$. The uncertainties in q are indicated by error bars and are a consequence of experimental errors in χ , T , and T_g and the uncertainties in the choices of the constants C and Θ . The critical index β was obtained using the relation

$$q(T) \propto (1 - T/T_g)^\beta \quad (5)$$

The values of β are 1.1 ± 0.2 and 1.0 ± 0.2 for χ_i [curve (b)] and χ_h [curve (a)] of Fig. 1, respectively. It should be noticed that this fitting is restricted only to one decade interval: $0.01 < (T_g - T)/T_g < 0.1$.

The value of β is in agreement with the prediction of mean-field theory: $\beta = 1.0$.^{5,17,18} It appears however to exclude the renormalization-group method prediction, obtained by Harris *et al.*¹⁹ They derived

expansions for the exponents in power of $\epsilon=6-d$, d is the dimension of the system, which leads in first order of ϵ to $\beta=2.5$ for the Ising model, 1.75 for the X - Y model and 1.6 for the Heisenberg model. It also excludes the prediction of the percolation theory by Kirkpatrick,²⁰ which gives $\beta=0.39$.

ACKNOWLEDGMENTS

Professor P.G. Winchell provided advice on the growth and heat treatment of the crystals. This work was supported by NSF Grant Nos. 76-80551 and NSF/MRL Program DMR 76-0889A1.

*On leave from Department of Physics, Faculty of Science, Hokkaido University, Sapporo, Japan.

¹V. Cannella and J.A. Mydosh, *Phys. Rev. B* **6**, 4220 (1972).

²J.L. Tholence and R. Tournier, *J. Phys. (Paris)* **35**, C4-229 (1974).

³N.C. Guy, *J. Phys. F* **7**, 1505 (1977).

⁴S.F. Edwards and P.W. Anderson, *J. Phys. F* **5**, 965 (1975).

⁵D. Sherrington and S. Kirkpatrick, *Phys. Rev. Lett.* **35**, 1792 (1975); S. Kirkpatrick and D. Sherrington, *Phys. Rev. B* **17**, 4384 (1978).

⁶T. Mizoguchi, T.R. McGuire, S. Kirkpatrick, and R.J. Gambino, *Phys. Rev. Lett.* **38**, 89 (1977).

⁷K. Binder; *Festkörperprobleme (Advances in Solid State Physics)*, Vol. XVII, edited by J. Treusch (Vieweg, Braunschweig, 1977), p. 55.

⁸J.A. Khan and D. Griffiths, *J. Phys. F* **8**, 763 (1978).

⁹J.S. Philo and W. M. Fairbank, *Rev. Sci. Instrum.* **48**, 1529 (1977).

¹⁰M. Cerdonio, F. Mogno, G.L. Romani, C. Messana, and C. Gramaccioni, *Rev. Sci. Instrum.* **48**, 300 (1977).

¹¹E.J. Cukauskas, D.A. Vincent, and B.S. Deaver, Jr., *Rev. Sci. Instrum.* **45**, 1 (1974).

¹²M. Cerdonio, C. Cosmelli, and G.L. Lomani, *Rev. Sci. Instrum.* **47**, 1 (1976).

¹³R.E. Sarwinski, *Cryogenics* **17**, 671 (1977).

¹⁴M. Cerdonio, R.H. Wang, G.R. Rossman, and J.E. Mercereau, in *Proceedings of the Thirteenth International Conference on Low Temperature Physics, 1972*, edited by K.D. Timmerhaus, W.J. O'Sullivan, and E.F. Hammel (Plenum, New York, 1974), Vol. IV, p. 525.

¹⁵E.P. Day, in Ref. 14, Vol. IV, p. 550.

¹⁶E.C. Hirschhoff, O.G. Symko, and J.C. Wheatley, *J. Low Temp. Phys.* **5**, 155 (1971).

¹⁷K.H. Fisher, *Phys. Rev. Lett.* **34**, 1438 (1975).

¹⁸D. Sherrington and B.W. Southern, *J. Phys. F* **5**, L49 (1975).

¹⁹A.B. Harris, T.C. Lubensky, and J.H. Chen, *Phys. Rev. Lett.* **36**, 415 (1976).

²⁰S. Kirkpatrick, *Phys. Rev. Lett.* **36**, 69 (1976).